

The Adenomatous Polyposis Coli Protein Is Required for the Formation of Robust Spindles Formed in CSF *Xenopus* Extracts[□]

Dina Dikovskaya, Ian P. Newton, and Inke S. Näthke*

Division of Cell and Developmental Biology, University of Dundee, WTB/MSI Complex, Dundee DD1 5EH, Scotland

Submitted August 20, 2003; Revised February 12, 2004; Accepted March 15, 2004
Monitoring Editor: Ted Salmon

Mutations in the adenomatous polyposis coli (APC) protein occur early in colon cancer and correlate with chromosomal instability. Here, we show that depletion of APC from cystostatic factor (CSF) *Xenopus* extracts leads to a decrease in microtubule density and changes in tubulin distribution in spindles and asters formed in such extracts. Addition of full-length APC protein or a large, N-terminally truncated APC fragment to APC-depleted extracts restored normal spindle morphology and the intact microtubule-binding site of APC was necessary for this rescue. These data indicate that the APC protein plays a role in the formation of spindles that is dependent on its effect on microtubules. Spindles formed in cycled extracts were not sensitive to APC depletion. In CSF extracts, spindles predominantly formed from aster-like intermediates, whereas in cycled extracts chromatin was the major site of initial microtubule polymerization. These data suggest that APC is important for centrosomally driven spindle formation, which was confirmed by our finding that APC depletion reduced the size of asters nucleated from isolated centrosomes. We propose that lack of microtubule binding in cancer-associated mutations of APC may contribute to defects in the assembly of mitotic spindles and lead to missegregation of chromosomes.

INTRODUCTION

Adenomatous polyposis coli (APC) is a tumor suppressor protein that is frequently mutated in colon cancer (Polakis, 1997). Due to the efforts of many laboratories, a role for APC in the regulation of β -catenin is well established (Bienz and Clevers, 2000; Polakis, 2001). Consistent with an important role for APC in affecting proliferation control, loss of APC has been established as a cause for the formation of polyps that invariably become malignant if left untreated (Fearhead *et al.*, 2001). However, APC mutations are detected at the earliest stage of polyp formation, 7–15 yr ahead of the manifestation of malignant carcinomas in patients (Boland and Kim, 1993). It is therefore likely that loss of APC at the early stage promotes tumor formation at least in part by a mechanism(s) that is independent of its activity as a regulator of β -catenin-mediated transcription and proliferation.

In support of this idea, it has been recently discovered that loss of wild-type APC correlates with chromosomal instability, a hallmark of colon polyposis (Fodde *et al.*, 2001; Kaplan *et al.*, 2001; Shih *et al.*, 2001). C-terminal APC truncations similar to those found in tumors correlate with chromosomal instability in mouse embryonic cells (Fodde *et al.*,

2001; Kaplan *et al.*, 2001). The molecular mechanism relating APC and chromosomal separation is not known.

APC has multiple, diverse binding partners. In addition to proteins involved in the regulation of β -catenin (such as β -catenin, axin, and GSK3 β), APC binds directly to microtubules (Deka *et al.*, 1998; Zumbunn *et al.*, 2001), to the microtubule binding protein EB1 (Su *et al.*, 1995; Juwana *et al.*, 1999), and interacts with the kinesin microtubule motor KIF 3a-3b via the adaptor protein KAP3 (Jimbo *et al.*, 2002). Furthermore, APC bundles and stabilizes microtubules in vivo and in vitro (Deka *et al.*, 1998; Zumbunn *et al.*, 2001). These data have established APC as a bona fide microtubule-associated protein, and this may relate to the mechanism of APC function in chromosome segregation. Based on the connections between APC and microtubules, we proposed that APC might regulate some aspects of formation and/or maintenance of mitotic spindles. Spindle defects caused by loss of functional APC could result in the missegregation of chromosomes in colon cancer cells, resulting in chromosomal instability and aneuploidy. Indeed, aberrant spindle structures have been reported in cells expressing mutant APC (Fodde *et al.*, 2001; Green and Kaplan, 2003). Consistent with a proposed role for APC in spindle function, APC localizes to different components of mitotic spindles: APC has been detected on kinetochores (Fodde *et al.*, 2001; Kaplan *et al.*, 2001) and in some cases on centrosomes (Kaplan *et al.*, 2001; Tighe *et al.*, 2001; Louie *et al.*, 2004).

Mitotic defects in tumor cells lines that express truncated APC have been examined previously (Fodde *et al.*, 2001; Tighe *et al.*, 2001; Green and Kaplan, 2003); however, the direct consequence of loss of APC has never been explored. Here, we investigate the relationship between loss of APC and spindle defects. We show that in *Xenopus* egg extracts arrested in metaphase of meiosis II (further referred to as

Article published online ahead of print. Mol. Biol. Cell 10.1091/mbc.E03-08-0613. Article and publication date are available at www.molbiolcell.org/cgi/doi/10.1091/mbc.E03-08-0613.

□ Online version of this article contains supporting material.

Online version is available at www.molbiolcell.org.

* Corresponding author. E-mail address: i.s.nathke@dundee.ac.uk.

Abbreviations used: APC, adenomatous polyposis coli; CSF, cystostatic factor.

“CSF [cytostatic factor] extracts”) depletion of APC results in a number of alterations in microtubule assemblies that form in these extracts. The DNA in CSF extracts is not replicated and thus these assemblies do not represent a true mitotic spindle. However, the actual organization of microtubules in these spindles resembles that in mitotic cells in many respects and thus they represent a valid model for studying mitotic spindle formation (Sawin and Mitchison, 1991; Desai *et al.*, 1999).

The defects we observed when APC was depleted included general loss of microtubule mass and redistribution of microtubule density from the center of spindles toward the poles. A direct effect of APC on spindle morphology was further confirmed by our result that recombinant APC protein rescues the APC-depleted phenotype and that the effect of APC on spindles is sensitive to the amount of APC present. Changes in CSF spindle structure that result from APC depletion can be attributed at least partially to direct effects on the microtubule network because APC removal also had an effect on asters formed in the absence of chromatin. Consistent with a role for APC in affecting spindle microtubules, we found that a portion of APC localized to spindle microtubules and the ability of APC to rescue CSF spindle formation required an intact microtubule-binding site. These data indicate the importance of APC–microtubule interactions for its role in spindle morphology in CSF extracts. Interestingly, we could not detect an effect of APC on spindles formed in cycled extracts. One explanation for this discrepancy may be the differences in the mechanism that govern spindle assembly in these two types of situations: in CSF extracts, spindle formation is predominantly initiated from asters, whereas in cycled extracts, microtubule polymerization is initiated from chromatin (Sawin and Mitchison, 1991). Our data provide the first evidence for a direct involvement of the tumor suppressor APC in spindle formation and reveal aster-nucleated microtubules as an important target of APC in mitosis.

MATERIALS AND METHODS

Preparation of Rhodamine-labeled Tubulin

Pig brain tubulin was prepared by two polymerization/depolymerization cycles and separated by phosphocellulose chromatography and labeled with tetramethyl-rhodamine (Molecular Probes, Eugene, OR) as described previously (Hyman *et al.*, 1991) followed by three cycles of polymerization and sedimentation through glycerol cushion to remove unbound fluorochrome and polymerization-incompetent tubulin. Labeled tubulin was resuspended in BRB80 (80 mM K-PIPES, pH 6.8, 1 mM MgCl₂, 1 mM EGTA) at ~20 mg/ml.

Preparation of Demembrated *Xenopus* Sperm Nuclei

Xenopus sperm nuclei were prepared as described previously (Murray, 1991) with the difference that for separation of sperm cells a Dounce homogenizer was used. Demembrated sperm nuclei were resuspended in NBP (250 mM sucrose, 15 mM K-HEPES, pH 7.4, 1 mM EDTA, 0.5 mM spermidine trihydrochloride, 0.2 mM spermine tetrahydrochloride, 1 mM dithiothreitol [DTT], 10 µg/ml leupeptin) containing 0.3% bovine serum albumin and 30% (wt/vol) glycerol at a final concentration of 3×10^7 sperm nuclei/ml.

Preparation of Mitotically Arrested *Xenopus* Egg Extract and Spindle Formation

CSF-arrested frog egg extracts were prepared following the guidelines described previously (Desai *et al.*, 1999; Swedlow, 1999). Only freshly prepared extracts were used for spindle formation. Spindles were formed in the presence of $1\text{--}3 \times 10^3$ demembrated sperm nuclei and ~0.4 µg of rhodamine-labeled pig brain tubulin per 1 µl of extract by incubating the mix for 40–60 min at room temperature. When needed, various dilutions of APC proteins or control vector in buffer containing 10 mM HEPES, pH 7.7, 1 mM MgCl₂, 100 mM KCl, and 150 mM sucrose were added to the spindle assembly reaction in a volume not exceeding 1/10 of the reaction volume.

For formation of spindles in cycled extracts, extracts were supplemented with 0.1 mg/ml creatine kinase, demembrated sperm nuclei, and rhoda-

mine-labeled tubulin at the same concentration as described above. Cycling was induced with 0.8 mM CaCl₂ and progression through interphase was monitored by examination of chromatin decondensation by using 4,6-diamidino-2-phenylindole (DAPI)-stained samples taken from the cycling extract. Sixty to 80 min after CaCl₂ addition extracts were driven into mitosis by addition of an equal volume of appropriate (mock- or APC-depleted) CSF extract supplemented with rhodamine-tubulin. Spindles were isolated onto coverslips as described below after 25–30 min.

Mitotic asters were prepared as described previously (Tirnauer *et al.*, 2002). Briefly, isolated centrosomes (kind gift from Dr. Jennifer Tirnauer, Harvard Medical School, Cambridge, MA) were added to 25 µl of CSF or cycled extracts containing rhodamine-labeled tubulin (Cytoskeleton, Denver, CO). After incubation for 5 or 10 min at room temperature, 20 µl of extract was diluted into 2 ml of BRB80 in 30% glycerol and mixed immediately. The mixture was overlaid on cushions of 4 ml of 40% glycerol in BRB80 and spun for 10' at $6000 \times g$ onto poly-lysine-coated coverslips. After washing the cushion interface repeatedly with BRB80/DTT, coverslips were fixed in methanol at –20°C and rehydrated in PBS. Coverslips were mounted onto glass slides and examined using a DeltaVision restoration microscope (Applied Precision, LLC, Issaquah, WA). For immunostaining of spindles, extracts were diluted and then fixed in 5% paraformaldehyde before sedimentation through a 40% glycerol cushion onto glass coverslips as described previously (Desai *et al.*, 1999; Swedlow, 1999). Primary antibodies were diluted 1:1000 for rabbit polyclonal anti-APC, 1:400 for anti-CenpE (kind gift from Dr. Don Cleveland, Ludwig Institute University of California, San Diego, CA) and 1:330 for Alexa-594-CenpA (a kind gift from Dr. Aaron Straight, Stanford University, Stanford, CA).

APC Immunodepletion

Protein A affi-prep beads (20 µl; Bio-Rad, Hercules, CA) or 100 µl of dynabeads slurry (DynaL Biotech, Lake Success, NY) were loaded with 30–40 µg of affinity-purified anti-APC antibody (Näthke *et al.*, 1996), mouse monoclonal affinity-purified anti-N-APC antibody O.T. 03 (Europa Bioproducts, Cambridge, United Kingdom), or the equivalent amount of rabbit or mouse IgG (Sigma-Aldrich, St. Louis, MO). Antibody-bound beads were washed three times in buffer containing 10 mM HEPES, pH 7.7, 1 mM MgCl₂, 100 mM KCl, 150 mM sucrose, and drained. Small aliquots (85–100 µl) of freshly prepared *Xenopus* egg extract were incubated with the antibody-bound beads for 1 h rotating slowly at 4°C. Beads were subsequently removed from depleted extracts using a Dynal MPC-S magnet or by centrifugation at $110 \times g$ as appropriate.

Immunoblots

Extracts were separated on 4–12% gradient SDS gels (MOPS running buffer; Invitrogen, Carlsbad, CA), by using 0.8 µl of extract per lane, and then transferred to Protran nitrocellulose membrane with 0.1-µm pore size (Schleicher & Schuell, Keene, NH). Primary antibodies were diluted in blocking solution (Tris-buffered saline containing 5% nonfat milk, 1% donkey serum, 0.02% Triton X-100) as follows: crude rabbit serum against the middle portion of APC, 1:1000; mouse monoclonal affinity purified anti-N-APC antibody O.T. 03, 1:500; anti-α-tubulin (DM1α; Sigma-Aldrich), 1:500; anti-EB1 mouse monoclonal antibody (kind gift from Jennifer Tirnauer, Harvard Medical School), 1:20,000; anti-XMAP310 mouse monoclonal antibody (kind gift from Eric Karsenti, European Molecular Biology Laboratory, Heidelberg, Germany), 1:1000; anti-XKCM1 rabbit polyclonal antibody (kind gift from Claire Walczak, University of Indiana, Bloomington, IN), 1:2000; anti-CENP-E tail II rabbit polyclonal antibody (kind gift from Don Cleveland, Ludwig Institute, San Diego, CA), 1:1000; and anti-XMAP215 rabbit polyclonal antibody (kind gift from Kazuhito Kinoshita, Max Planck Institute, Dresden, Germany), 1:500. Secondary anti-rabbit or anti-mouse horseradish peroxidase-labeled antibodies (Scottish Antibody Production Unit, Carluke, Scotland, United Kingdom) were diluted 1:5000.

Histone 1 Kinase Assay

Snap-frozen extract was diluted 75-fold (vol/vol) in EB buffer (80 mM Na β-glycerophosphate, pH 7.3, 10 mM MgCl₂, 5 mM EGTA, 1 mM DTT) containing protease inhibitors: 0.5 mM phenylmethylsulfonyl fluoride, 10 µg/ml leupeptin, 10 µg/ml pepstatin A, 10 µg/ml chymostatin, and 1 mM phosphatase inhibitor Na₃VO₄. Histone H1 (0.4 µg; Roche Diagnostics, Mannheim, Germany) (final concentration 0.2 mg/ml) was phosphorylated in the presence of 10 µl of extract-EB dilution, 20 mM HEPES, pH 7.2, 10 mM MgCl₂, 5 mM EGTA, and 0.2 mM ATP containing [γ -³²P]ATP to ~0.45 µCi/nmol ATP, for 10 min at room temperature, in a total volume of 20 µl. The reaction was stopped by boiling in reducing sample buffer (2% SDS, 50 mM DTT, 40 mM Tris-HCl, pH 6.8, 10% glycerol). The reaction mix was separated by PAGE, and the gel was exposed to Konica Medical film.

Cloning and Production of APC Fragments

APC4 and APC4ΔMT, the fragments of APC containing the middle and C-terminal portion (nucleotides 3080–8573 corresponding to residues 1015–2843 of human APC), were amplified by polymerase chain reaction from the

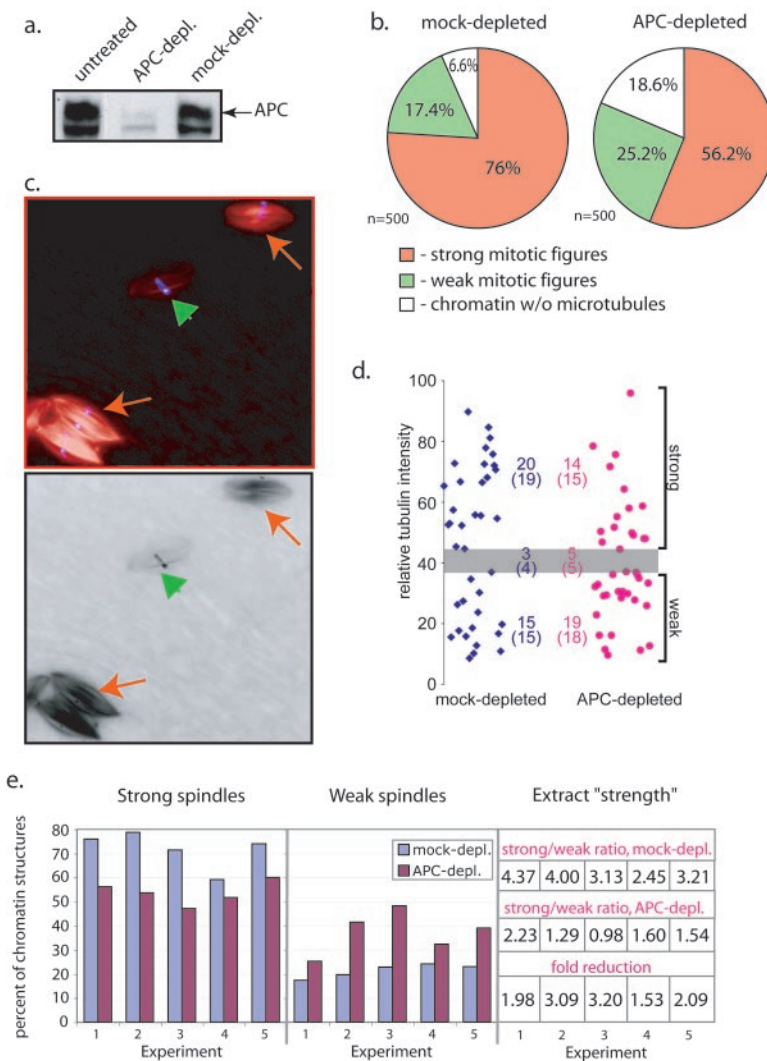


Figure 1. APC depletion weakens mitotic spindles in *Xenopus* egg extract. (a) Immunoblotting of *Xenopus* egg extract, either untreated or immunodepleted with affinity-purified anti-APC antibody or rabbit IgG as indicated, shows significant depletion of APC only when anti-APC antibody was used. We always detected three bands in *Xenopus* egg extracts that are reactive with our anti-APC antibody. Only the upper band was also detected by other APC antibodies. This band has the correct size and is therefore considered to represent full-length APC. The middle band seems to be partially removed during APC depletion, whereas the bottom band does not change after depletion. (b) The proportions of strong (orange) and weak (green) mitotic figures (bipolar spindles and asters) and microtubule-free-chromatin (white) found in mock- and APC-depleted extracts were measured using 500 nuclei for each extract condition. APC depletion resulted in a decrease in the proportion of strong mitotic figures compared with mock-depleted control. These data corresponds to experiment 1 in e. (c) Examples of spindles formed in *Xenopus* egg extract in the presence of sperm nuclei chromatin (blue) and rhodamine-labeled tubulin (red) reflect the heterogeneity in the types of spindles found even in untreated extracts. High intensity (strong, red arrows) and low intensity (weak, green arrowhead) spindles were found next to each other in the optical field, reflecting the natural variability in the microtubule content of such spindles. (d) Images of a randomly selected set of spindles collected from mock- or APC-depleted extracts were recorded and the total tubulin intensity was measured using NIH Image software. The scatter chart represents the mean tubulin intensities of individual spindles found in mock-depleted (blue) and APC-depleted (pink) extracts. These spindles were independently scored visually as described in Figure 1b (numbers in brackets) and the gray zone depicts the range of intensities of those spindles that were scored as ambiguous by the visual examination. Using this zone to define a threshold, strong and weak spindle populations could be counted based on their measured intensities and these are shown in the chart (upper numbers). Note that the numbers obtained by these two methods are practically identical. (e) This diagram shows the proportion of strong (left) and weak (middle) spindles in mock- (blue) and APC-depleted (purple) extracts from five independent experiments. Extract

strength was calculated as a ratio between strong and weak mitotic figures formed in the extracts as shown on the table. Fold reduction of extract strength from mock-depleted to corresponding APC-depleted extracts provides a numeric representation of the weakening of spindles upon APC depletion (lower line). This allows a direct comparison of a number of independent experiments. The fold reduction was reproducibly larger than 1, and averaged 2.37 ± 0.73 , indicating that APC depletion always produced weaker spindles, independently of the initial strength of the extract. For each experiment, 300–500 spindles were scored for mock- and APC-depleted samples.

pEGFP-C3 vector containing full-length APC or full-length APC with deletion in its microtubule-binding domain, respectively (Zumbrunn *et al.*, 2001). The primers used were designed to introduce BspE1 and BamHI restriction sites and a FLAG tag at the 5' end (5'-GCGCGC TCCGGA GGATCC ATGGAC TACAAG GACGAC GATGAC AAGGAT GATAAT GATGGA GAACTA GATACA-3') and a SacI restriction site at the 3' end (5'-GCGCGC GAGCTC TTAAC AGATGT CACAAG GTAAGA CCCAGA-3'). By using the BamHI/SacI sites, the fragments were inserted into pFB-NHis10HA plasmid (a kind gift from Aurora Burds, Massachusetts Institute of Technology, Cambridge, MA), a derivative of pFastBac plasmid with a modified multiple cloning site that introduces 10× His tags and one hemagglutinin (HA) tag at the N terminus of the fusion protein. The pFastBac plasmid containing full-length APC (a kind gift from Joanna Groden, University of Cincinnati, Cincinnati, OH), as well as pFB-Nhis10HA containing APC4 were transfected into competent DH10Bac bacteria, and the baculoviruses carrying the APC constructs were produced in Sf 21 cells following the instructions in the Bac-to-Bac Baculovirus expression manual (Invitrogen). APC proteins were purified using Ni²⁺-agarose as described in QIAGEN (Valencia, CA) protocol.

Microscopy

Spindle assembly reaction (2 μl) was transferred onto a glass slide, fixed with 4 μl of 4% formaldehyde solution, containing 60% (vol/vol) glycerol, 1× MMR (100 mM NaCl, 2 mM KCl, 1 mM MgCl₂, 2 mM CaCl₂, 0.1 mM EGTA, 5 mM HEPES pH 7.8), 1 μg/ml DAPI, and covered with a coverslip. These

squashes were analyzed using a 20×/0.7 numerical aperture (NA) or 40×/0.85 NA lens on a Leica DMIRB microscope operated by Improvision Openlab 3.0 software. Images were captured with a Hamamatsu ORCA camera.

The high-resolution images shown in Figures 2b, 6, and 8 and in Supplemental Figure 5 and 6 were collected and analyzed using a Delta Vision Restoration Imaging System (Applied Precision) built on a Nikon inverted microscope by using 100×/1.4 NA objective lens.

Measurements of Microtubule Intensity and the Length of the Spindles

Images used to quantitate tubulin intensity were collected on the Leica microscope. Images were transferred from Openlab to NIH Image 1.62f, and the mean intensity in each spindle and aster was measured after background subtraction. Intensity values were then adjusted for exposure time if necessary.

The images used to analyze the tubulin distribution were collected on the Leica microscope and then transferred from Openlab 3.0 to NIH Image 1.62f software. Randomly selected single bipolar spindles were analyzed (asters or clusters of spindles were ignored). Vertically positioned and manually outlined spindle images were analyzed for the distribution of intensity along the spindle axis by using the programmable "macro" command that scans along the Y coordinates of the image of the spindle and returns the average intensity of the slice across each pixel of the Y coordinate. This analysis also provides

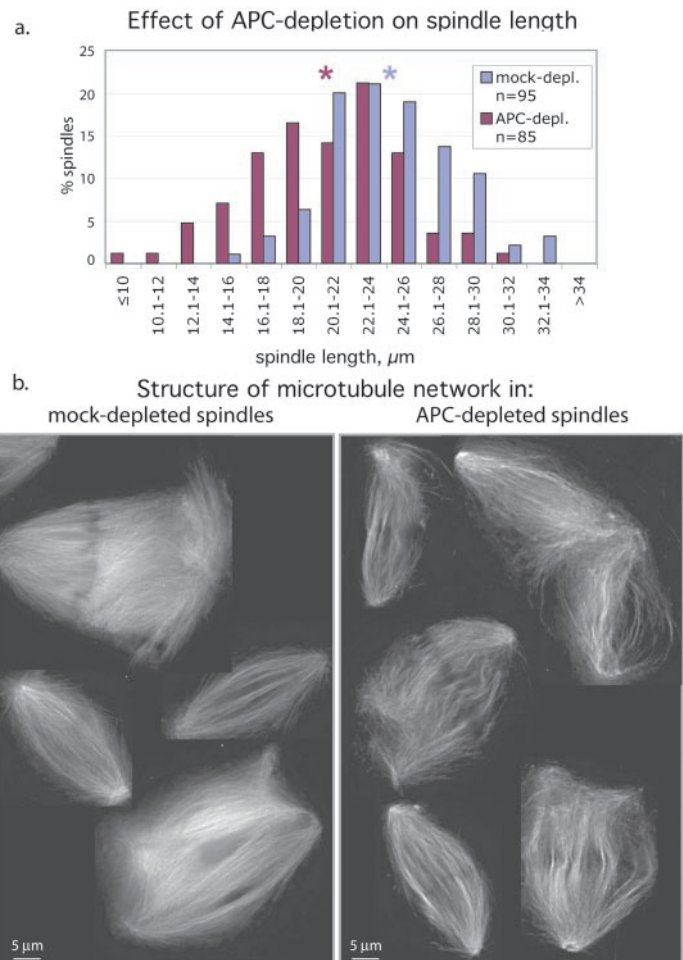


Figure 2. Removal of APC affects spindle length and fine structure of microtubule network. (a) Pole-to-pole distance was measured in spindles formed in mock- or APC-depleted extracts. The histogram represents the distribution of spindles according to their length in micrometers. Stars mark the average spindle length for each type of extract. (b) Single optical sections ($0.2 \mu\text{m}$) of microtubules in spindles formed in mock- and APC-depleted extracts (as indicated) revealed less tightly packed and curved microtubule bundles in spindles formed in the absence of APC.

information about the length of the spindle. The full text of the macro program can be provided upon request. The background-corrected data were then placed into Microsoft Excel and processed as follows.

Each set of data representing one spindle was divided into 10 groups, corresponding to 1/10 of the spindle length. For every such group, the average intensity was calculated. These "10 step values" were normalized to the total average intensity of the spindle, which was set to 100%. This type of "spindle data" from one extract (APC or mock depleted) was used to calculate the averages that are plotted in Figure 3c. The curves represent the normalized distribution of intensity (=tubulin density) along the length of the average APC- or mock-depleted spindle, with centrosomal regions at the ends and kinetochore region in the middle of the curve.

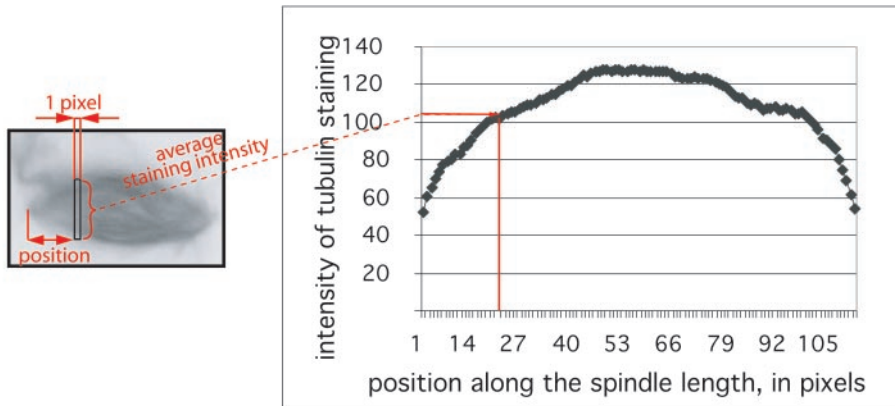
RESULTS

Spindles Formed in the Absence of APC Have a Less Robust Morphology

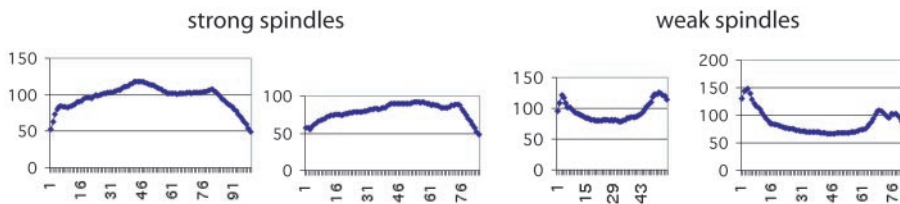
To determine whether APC is involved in spindle formation, we specifically immunodepleted APC from *Xenopus* egg extracts arrested at metaphase of meiosis II (CSF extract) (Figure 1a) and allowed spindles to form in the presence of *Xenopus* sperm chromatin and rhodamine-labeled tubulin. For comparison, control, mock-depleted extracts were generated using purified rabbit IgG. To measure differences between spindles formed in the presence and absence of APC, we classified spindles and asters (further referred collectively as mitotic figures) into "strong" and "weak." This classification was based on the general fluorescent intensity of the incorporated labeled tubulin above background. As shown in the example in Figure 1c, even in untreated control

extracts spindles vary greatly in fluorescent intensity but can be subdivided into the two general categories shown in Figure 1c. For each experiment a threshold between weak and strong spindles was established visually, so that the majority of normal looking spindles in mock-depleted extract could be classified as strong. All other samples from the same experiment were then scored using the same threshold. Using this method, we counted the numbers of strong and weak mitotic figures as well as chromatin that was not associated with microtubules. In each experiment, there were a small number of mitotic figures ($\leq 10\%$) that were intermediate in intensity and could not be classified unambiguously. These were scored separately, and the value divided equally between the strong and weak counts. For each condition, 300–500 randomly selected mitotic figures were scored. This large number precluded recording individual images for all mitotic figures that were scored. To ensure that the classification was not biased, we used a small sample of randomly selected spindles for more objective measurements. We recorded 41 randomly selected mitotic figures from each type of sample and quantitated their mean fluorescence intensity (Figure 1d). The intensity value for those spindles in this data set that had been classified as ambiguous in the visual inspection was set as the threshold between weak and strong (Figure 1d, gray bar) to differentiate between strong and weak spindles. The results obtained with this analysis were indistinguishable from those

a. Measurement of distribution of tubulin density along the spindle



b. Examples of tubulin density distribution in:



c. Average distribution of tubulin density along spindles

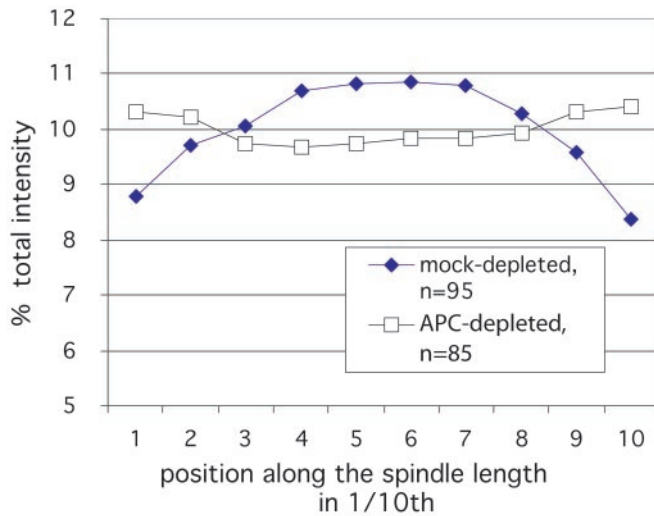


Figure 3. Distribution of tubulin in mitotic spindles is altered by APC-depletion. Spindles were allowed to form in APC- or mock-depleted extracts in the presence of rhodamine-labeled tubulin. Fluorescent images of tubulin in the spindles were captured and analyzed in the following manner. (a) Each spindle image was scanned along its length from one pole to another, and the average intensity of tubulin staining in a slice across the spindle axis was taken at each pixel position. This intensity was plotted against position along the pole-to-pole axis for each slice. (b) Examples of individual measurements performed as in panel a are shown for strong and weak spindles. These examples show the raw data without normalization for length or overall spindle intensity. (c) Measurements were performed as described in panel a by using 95 randomly selected mock-depleted (blue diamonds) and 85 APC-depleted (white squares) spindles. Intensities in each segment along the spindle axis were normalized to overall mean spindle intensity and these values were plotted against relative position along the pole-to-pole axis.

obtained by the “manual” classification (Figure 1d), confirming that our manual classification of spindles as weak and strong is a valid method to evaluate the difference in spindles.

The proportion of strong and weak mitotic figures, as well as chromatin structures that were not associated with any microtubules, were counted in APC-depleted and mock-depleted extracts (Figure 1b). These numbers were used to calculate the ratio between strong and weak figures, defined here as extract “strength.” Due to the inherent variability in the quality of extracts prepared on different days, there was variation in extract strength in different mock-depleted extracts (Figure 1e). However, APC depletion reproducibly

resulted in a shift toward the formation of weak mitotic spindles (Figure 1e) and reduced extract strength by comparable amounts in several independent experiments (Figure 1e). On average, extract strength in APC-depleted extracts was decreased 2.4-fold in comparison with corresponding mock-depleted extracts (from 5 experiments, SD = 0.7). The difference in the amount of microtubule-free chromatin between APC- and mock-depleted extracts was not reproducibly different between experiments.

Similar results were obtained with a monoclonal anti-APC antibody directed against a different epitope (O.T. 03; Europa Bioproducts) that could deplete APC as efficiently as the polyclonal antibody used in the experiments shown.

Figure 4. The ability of recombinant APC to rescue APC-depleted extracts requires the major microtubule-binding site of APC. Spindles were formed in APC-depleted or mock-depleted extracts supplemented with the indicated APC proteins or control buffer. The number of strong and weak mitotic figures was counted and the ratio between them was calculated for each extract condition. The number of spindles counted for each condition is indicated in brackets. (a) Fractions from SF21 cells that had been infected with either baculovirus encoding His-tagged full-length APC (lanes 2 and 4) or control vector (lanes 1 and 3) were eluted from Ni²⁺-agarose and subjected to SDS gel electrophoresis. Gels were stained with Coomassie (lanes 1 and 2) or blotted to membranes and probed with a mouse monoclonal anti-APC antibody (lanes 3 and 4). (b) Immunoblot of mock- (lanes 1 and 3) or APC-depleted (lanes 2 and 4) extracts after addition of fractions containing either vector control (lanes 1 and 2) or full length APC (lanes 3 and 4) was performed using antibodies against APC. This confirmed that the amount of full-length APC added was slightly below that of endogenous APC. Tubulin antibodies were used to verify equal loading. The table summarizes the ratio between strong and weak mitotic figures for each extract condition. Note that addition of APC to APC-depleted extracts restores this ratio to that of mock-depleted extracts to which control buffer had been added. Note also that addition of APC to mock-depleted extracts weakened spindles. (c) Coomassie-stained gel of 1 μ g of purified APC4 and 0.6 μ g of APC4 Δ MT. (d) Immunoblot (top) of mock- or APC-depleted extracts as indicated, supplemented with APC4 (lane 3 and 6), APC4 Δ MT (lane 2 and 5) to bring the final protein concentration of exogenous APC to 0.5 ng/ μ l, or control buffer (lane 1 and 4), were probed with anti-APC antibody to confirm that the amount of APC4 that was added was similar to that of endogenous APC. Antibodies against α -tubulin were used on the same blot to confirm equal protein loading. The table (bottom) shows the ratio between strong and weak mitotic figures for each combination revealing that addition of APC4 but not APC4 Δ MT rescued the effect of APC depletion. Note that addition of APC4 to mock-depleted extracts caused a significant decrease in spindle strength. (c, d, g, and h) Images of spindles from the experiments outlined above illustrate the effect of fl-APC (d) or APC4 (h) on the morphology of spindles formed in APC-depleted extracts (c and g).

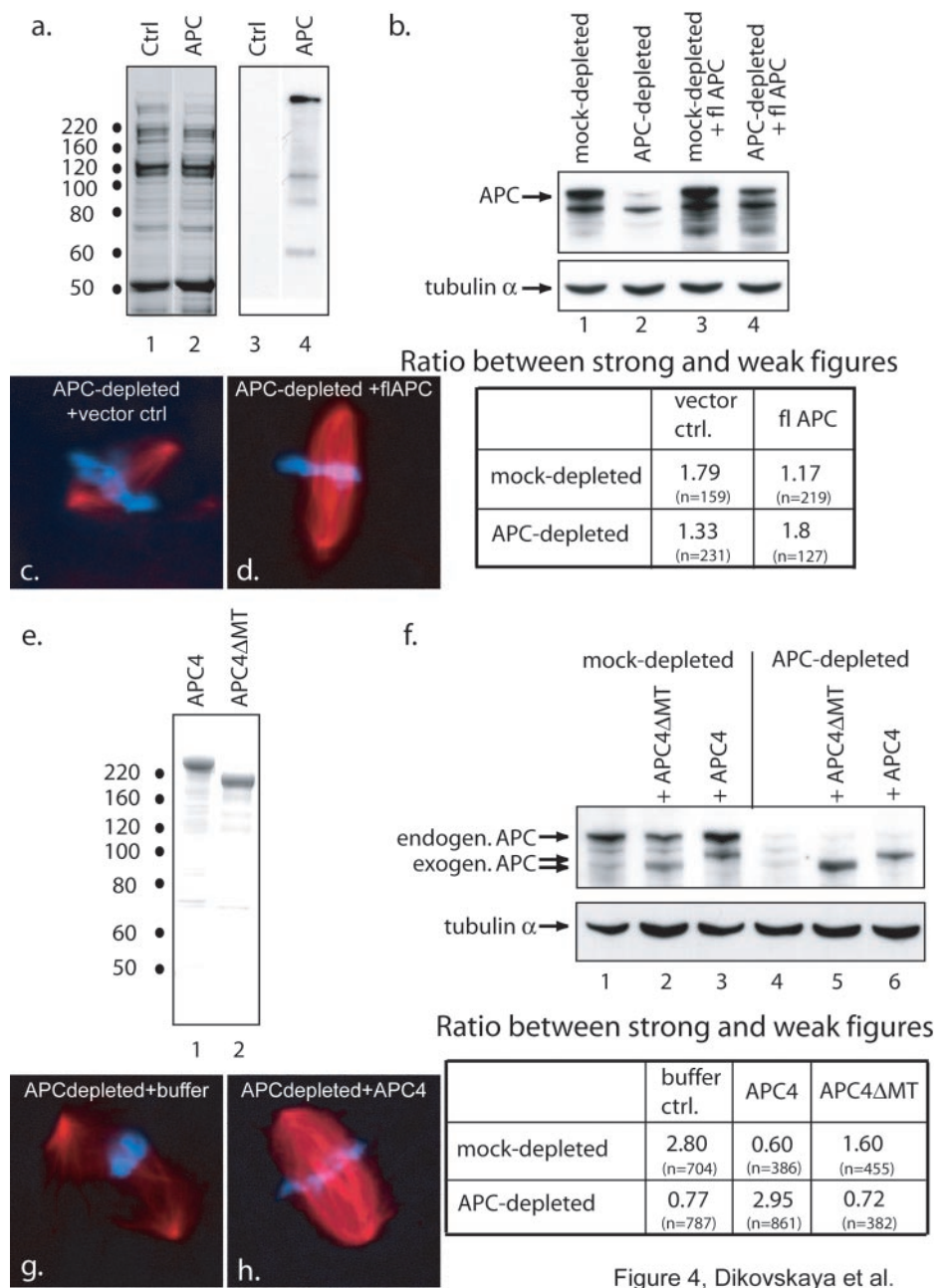


Figure 4, Dikovskaya et al.

These data suggest that spindles formed in the absence of APC contain less tubulin.

Closer examination of these spindles revealed that spindles formed in APC-depleted extracts were shorter than those formed in mock-depleted extracts as shown in the histogram in Figure 2a. The average spindle length dropped from $24.2 \pm 3.7 \mu\text{m}$ in mock-depleted extract to $20.7 \pm 4.4 \mu\text{m}$. High-resolution images of single $0.2\text{-}\mu\text{m}$ optical sections of spindles formed in different extracts further showed that the fine structure of the microtubule network in spindles formed in APC-depleted extract differed from that in control spindles (Figure 2 b). Control spindles contained

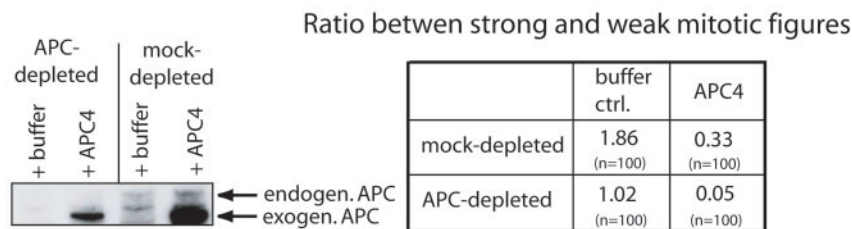
many more microtubules that looked continuous and straight, whereas microtubule bundles in APC-depleted spindles were wavy and less tightly packed.

These results suggested that removal of endogenous APC "weakens" spindles formed in CSF extracts so that they contain fewer microtubules and the structural organization of the spindle microtubule network is less robust.

The Distribution of Tubulin in CSF Spindles Is Altered When APC Is Absent

We noticed that in weak spindles, which predominated in APC-depleted extracts, the tubulin distribution seemed to be

a.



b.

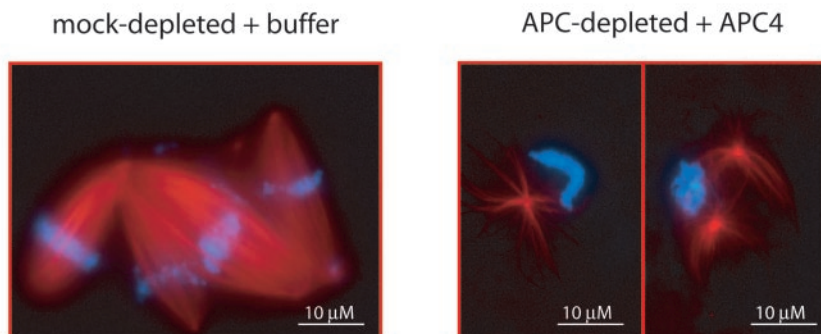


Figure 5. Excess APC is deleterious for spindle formation. (a) Immunoblot (left) of APC- (lanes 1 and 2) or mock-depleted (lanes 3 and 4) extracts after addition of a 4–5 fold excess of APC4 over level of endogenous APC (~2.3 ng/ μ l final concentration) (lane 2 and 4) or buffer alone (lane 1 and 3) using APC antibodies. The table on the right shows the ratio between strong and weak mitotic figures for each condition. Addition of an excess of APC4 results in significant weakening of spindles in both mock and APC-depleted extracts. (b) Representative examples of mitotic figures from the experiment shown in a. In APC-depleted extracts supplemented with APC4 in four- to fivefold excess of endogenous APC, most spindles were abnormal and contained very little tubulin compared with the robust, strong spindles that predominated in the control extracts.

altered such that most of the tubulin was concentrated at spindle poles and not in the center of the spindle as in the strong spindles, which are more common in control extracts. To quantitate this difference, we measured the average fluorescence intensity of rhodamine-labeled tubulin in individual, one pixel-wide cross sections along the spindle axis for each spindle (Figure 3a).

This analysis confirmed that in weak spindles there was relatively more tubulin near the poles and less tubulin at the center compared with strong spindles as shown in the individual examples in Figure 3b. To analyze data from spindles of different sizes and overall intensity, the total intensity for each spindle was set to 100%. Spindle axis length was divided into ten equal segments and the relative contribution of the intensity in each of these segments was calculated. Calculating the average of this type of data for 95 mock-depleted and 85 APC-depleted spindles that were randomly selected confirmed that the peak of tubulin intensity in APC-depleted spindles was shifted away from the center of spindles toward spindle poles (Figure 3c). This measurement provided an additional objective means to compare control and APC-depleted spindles because all the spindles generated in mock- and APC-depleted extracts were used to calculate the averages shown in Figure 3c (i.e., there was no selection or classification). The change in the average distribution of tubulin along the spindle axis in an entire population of spindles further confirmed that spindle structure is altered in the absence of APC.

Rescue of APC Depletion Defects Can Be Achieved by Addition of Endogenous Levels of APC Protein

We were able to exclude codepletion of important spindle and microtubule regulators with APC such as XMAP215, XKCM1, XMAP310, EB1, and CenPE as a contributing factor to the spindle abnormalities in APC-depleted extracts (see Supplemental Material). We also confirmed that APC depletion did not override the CSF arrest because it did not cause

premature decrease in mitotic kinase activity and did not result in changes in overall chromatin morphology (see Supplemental Material). To discriminate further between direct and indirect effects of APC depletion on spindle formation, we measured the ability of purified recombinant APC to rescue the APC-depletion phenotype.

Full-length human APC was expressed as a His-tagged fusion protein and partially purified using Ni²⁺-agarose (Figure 4a). Spindle formation was measured in APC-depleted and mock-depleted extracts with and without addition of crude fractions containing recombinant APC. To control for possible buffer effects, Ni²⁺-agarose eluate of lysate from SF21 cells expressing empty vector was used as “vector control” (Figure 4a). Addition of full-length APC, but not empty vector control, reversed the effect of APC depletion (Figure 4, c and d) as confirmed by a shift in the ratio between strong and weak spindles back to the level in mock-depleted extract (Figure 4b). These data confirmed that APC plays a direct role in spindle formation. Unfortunately, addition of the elution buffer on its own compromised the extract at the dilution that had to be used to achieve levels of exogenous APC similar to endogenous levels. As a consequence, the effect of APC depletion on these extracts was not as striking (compare the ratio of strong to weak spindles in APC depleted and mock depleted in vector control extracts in Figure 4b with Figure 1e). However, the improvement that was achieved by adding partially purified APC to extracts depleted of APC was reproducible. To overcome the potentially hampering effect of the elution buffer, we used a large N-terminally truncated fragment of APC (APC4) that we could prepare significantly more pure and concentrated (Figure 4e), so that buffer effects and contamination with other proteins and degradation products could be kept to a minimum. In a series of pilot experiments, we established that adding recombinant APC4-10 to nM produced a concentration that was similar to

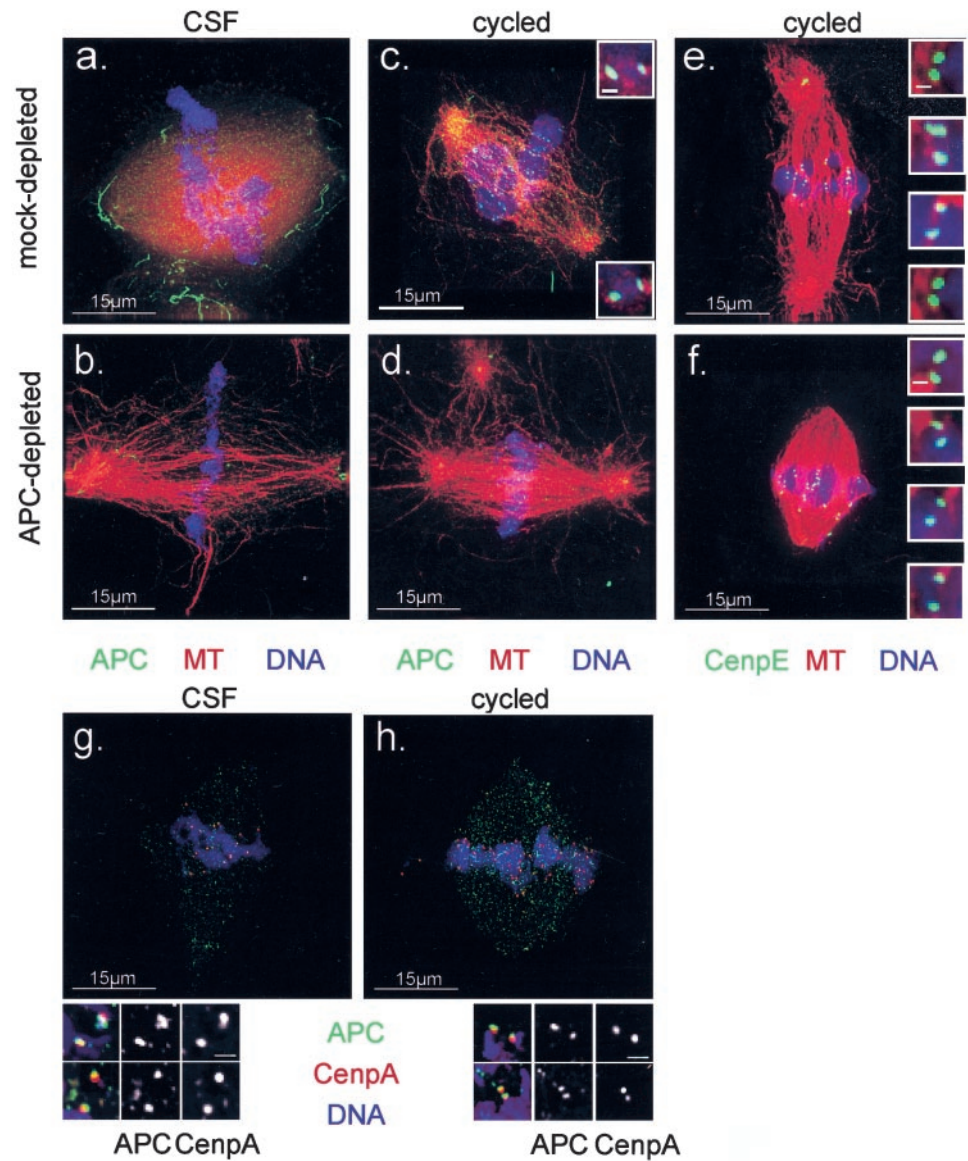


Figure 6. APC localizes to mitotic spindles and kinetochores in *Xenopus* extracts. Spindles were prepared in mock (a, c, e, g, and h) or APC-depleted (b, d, and f) CSF (a, b, and g) or cycled (c, e, d, f, and h) extracts and sedimented onto coverslips before fixing and staining with DAPI (blue) and antibodies against APC (indicated in green) (a–d, g and h), CenpE (e and f), or CenpA (g and h) as indicated. Tubulin is shown in red. Images were collected using a DeltaVision restoration microscope and represent volume projections of the entire spindle thickness. Images of mock- and APC-depleted spindles from the same extracts (a–d) were collected using identical settings for the image collections and processing. Insets in c, e, f, g, and h represent single 0.2- μm optical sections. APC was enriched at spindle poles but also decorated the entire microtubule lattice. In addition, APC accumulated in dot-like structures that are paired in cycled spindles and resemble kinetochores labeled with CenpE antibodies (e and f). APC in these structures costained with antibodies against CenpA (g and h). As expected, staining was significantly reduced after APC-depletion. Bar in insets, 0.5 μm (c, e, and f) and 1 μm (g and h).

that of endogenous APC. Addition of this amount of APC4 to APC-depleted extracts rescued spindle defects (Figure 4, f–h). The ability of purified APC protein or its fragments to rescue spindle morphology supports our conclusion that APC is one of the factors that is directly involved in establishing correct spindle structure.

Microtubule Binding of APC Is Essential for Its Ability to Support the Formation of Robust Mitotic Spindles

To test whether the function of APC in spindle formation requires its direct interaction with microtubules, we used the same N-terminally truncated APC fragment as described above lacking the major microtubule-binding site (APC4 Δ MT). This form of APC does not bind strongly to microtubules (Zumbrunn *et al.*, 2001). Deleting the major microtubule binding site from the fragment of APC rendered it unable to rescue the APC-depletion phenotype (Figure 4f). This confirmed that the ability of APC to bind microtubules directly is essential for its effect on CSF spindles.

APC in Excess of Endogenous Levels Disrupts Spindles

Addition of APC in significant excess of endogenous APC had deleterious effects on spindles. The ratio of strong to weak mitotic figures was decreased dramatically when APC4 was added in approximately fivefold excess over endogenous to either mock- or APC-depleted extract (Figure 5). The spindles observed in such extracts were largely abnormal as shown in the examples in Figure 5b. Mock-depleted control spindles produced in the same experiment and captured at the same time point looked normal (Figure 5b). We concluded that the exact stoichiometry between APC and other factor(s) in the extract are crucial for proper spindle formation. This was further confirmed by our observations that addition of APC or APC4 to mock-depleted extracts to raise the APC level above endogenous, always caused spindle weakening (tables in Figures 4 and 5).

APC Localizes to Mitotic Spindles in *Xenopus* extracts

The above-mentioned experiments clearly indicated that APC is necessary for formation of robust spindles in *Xenopus*

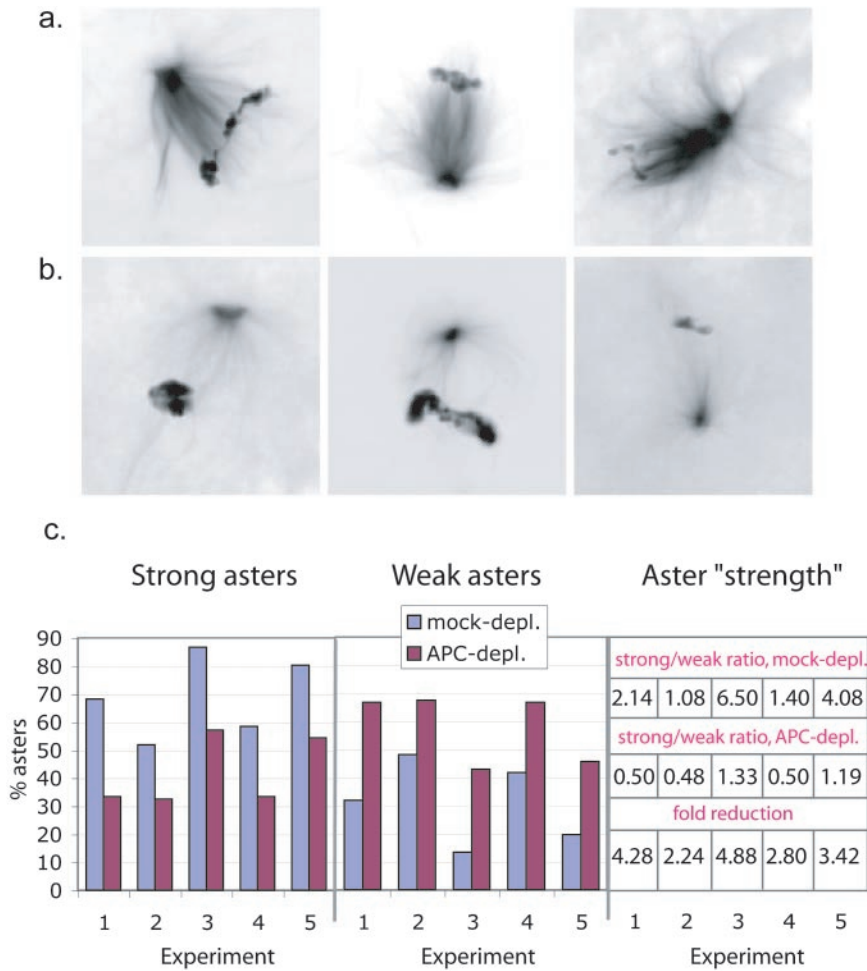


Figure 7. Depletion of APC results in defects in asters. Asters formed in mock- and APC-depleted *Xenopus* CSF extracts in the presence of sperm nuclei were scored as strong (a) or weak (b) based on general tubulin intensity (exactly as in Figure 1). (c) The proportion of strong asters was significantly reduced in extracts after APC depletion. The bar diagram shows the proportion of strong (left) and weak (middle) asters in mock- (blue) and APC-depleted (purple) extracts in 5 independent experiments. Aster "strength" was calculated as the ratio between strong and weak asters and is shown in the table on the right. Fold reduction of the aster strength from mock-depleted to corresponding APC-depleted extracts (lower line) was reproducibly greater than 1, average 3.52 ± 1.07 , indicating that APC depletion had a robust weakening effect on asters.

egg extract. To identify the site of action of APC within spindles, we determined the localization of APC in spindles formed in CSF and cycled extracts (Figure 6). The distribution of APC in the two types of spindles was similar: spindle microtubules were decorated with APC in a punctate pattern (Figure 6). In addition, APC was concentrated in tube-like structures near the pole, particularly in CSF spindles (Figure 6, a and g). APC was also detected in chromatin-associated dots in CSF and similar pairwise dots in cycled spindles (Figure 6c) that looked similar to kinetochores marked by Cenp-E (Figure 6, e and f). Double staining with antibodies against APC and a directly labeled anti-CenpA antibody (Figure 6, g and h) revealed that a portion of APC colocalized with CenpA in both CSF and cycled extracts. It confirmed the presence of APC at kinetochores or kinetochore-like structures in spindles assembled in *Xenopus* egg extracts. The signal for APC was significantly reduced in spindles formed in APC-depleted extracts at all these sites. Some of the residual staining we detected may be due to incomplete depletion (Figure 6, b and d). Alternatively, it is possible that chromatin-associated APC was reintroduced to extracts by the addition of chromatin.

APC Depletion Affects Aster Formation

Our experiments revealed altered microtubule networks in APC-depleted spindles and showed that the microtubule-binding site of APC was required for its ability to rescue these changes. In addition, APC can directly affect microtu-

bule stability in interphase (Zumbrunn *et al.*, 2001). Combined these observations are consistent with the idea that APC is involved in stabilizing spindle microtubules. Based on its localization in spindles, APC could participate in specifically stabilizing microtubules at kinetochores and/or it could also affect the entire microtubule network throughout the spindle. Although it is unlikely that CSF spindles have fully functional kinetochores (Sawin and Mitchison, 1991), the localization of CenpA (Figure 6), CenpE, and XKCM1 (our unpublished data) to highly focused spots on chromosomes in these extracts suggests that CSF spindles assemble some kinetochore-like complex. To determine whether APC affects spindle microtubules independently of its potential effect on such structures, we asked whether APC removal had an effect on the early stages of spindle formation when microtubule connections with chromatin are not yet well established. In our CSF-arrested *Xenopus* egg extracts, this early stage was represented by asters formed in the vicinity of and polarized toward chromatin (Figure 7, a and b; also see Figure 10). We counted the number of weak and strong asters by using the same criteria as described above in Figure 1 in APC- and mock-depleted extracts. We found that APC removal reproducibly resulted in a large increase in the proportion of weak asters (Figure 7c). These data suggested that APC plays a role in early stages of spindle formation in CSF extract.

It has been recently demonstrated that chromatin can influence aster outgrowth without direct contact between

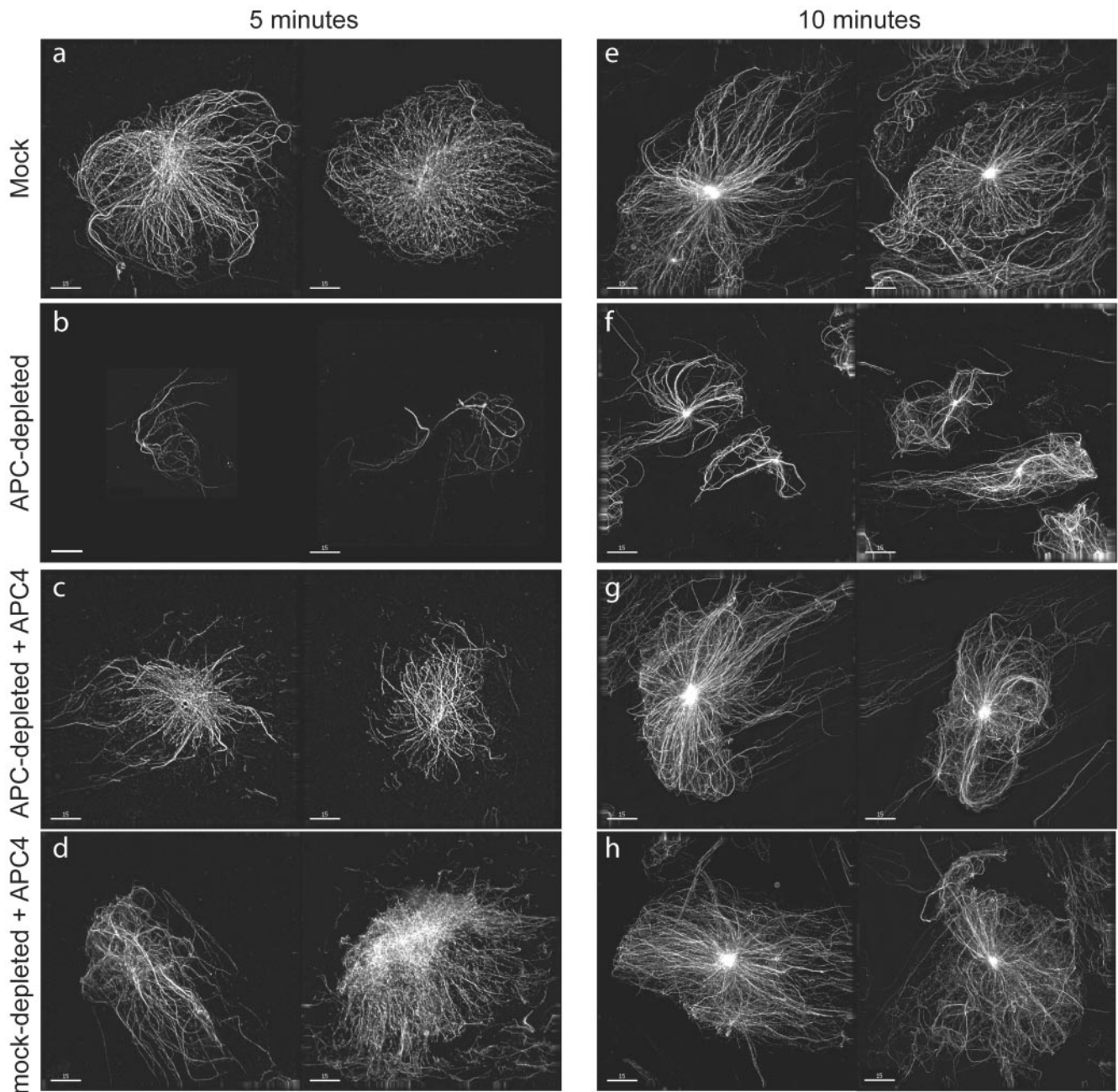


Figure 8. Depletion of APC compromises the formation of asters. Asters nucleated from isolated centrosomes in mock-depleted (a, d, e, and h) or APC-depleted (b, c, f, and g) CSF extracts that did (c, d, g, and h) or did not contain APC4 (a, b, e, and f) as indicated, were sedimented onto glass coverslips 5 (a–d) or 10 min (e–h) after initiation of tubulin polymerization. Asters were imaged using a DeltaVision restoration microscope. Images of two examples of typical asters obtained in the indicated conditions are shown. APC depletion reduced aster size, and this effect was rescued by addition of the APC4 fragment. Bar, 15 μm .

microtubules and chromatin structures (Carazo-Salas and Karsenti, 2003). To determine effects of APC on microtubules in the absence of any impact from chromatin, we nucleated asters from isolated centrosomes (Figure 8). In CSF extracts, depletion of APC resulted in the formation of asters that were significantly smaller than those formed in mock-depleted control extracts (Figure 8). Importantly, addition of the APC4 fragment reversed the effect of APC-depletion, and further increased the size of asters formed in mock-depleted extracts (Figure 8). These data confirmed the direct

involvement of APC in promoting the outgrowth of aster microtubules, suggesting that at least part of the spindle defects that resulted from APC depletion can be explained by its direct effects on microtubules.

APC Depletion Does Not Weaken Cycled Spindles

To gain further insights into the mechanism that governs the role of APC in spindle formation, we compared spindles formed in CSF and cycled extracts. We counted weak and

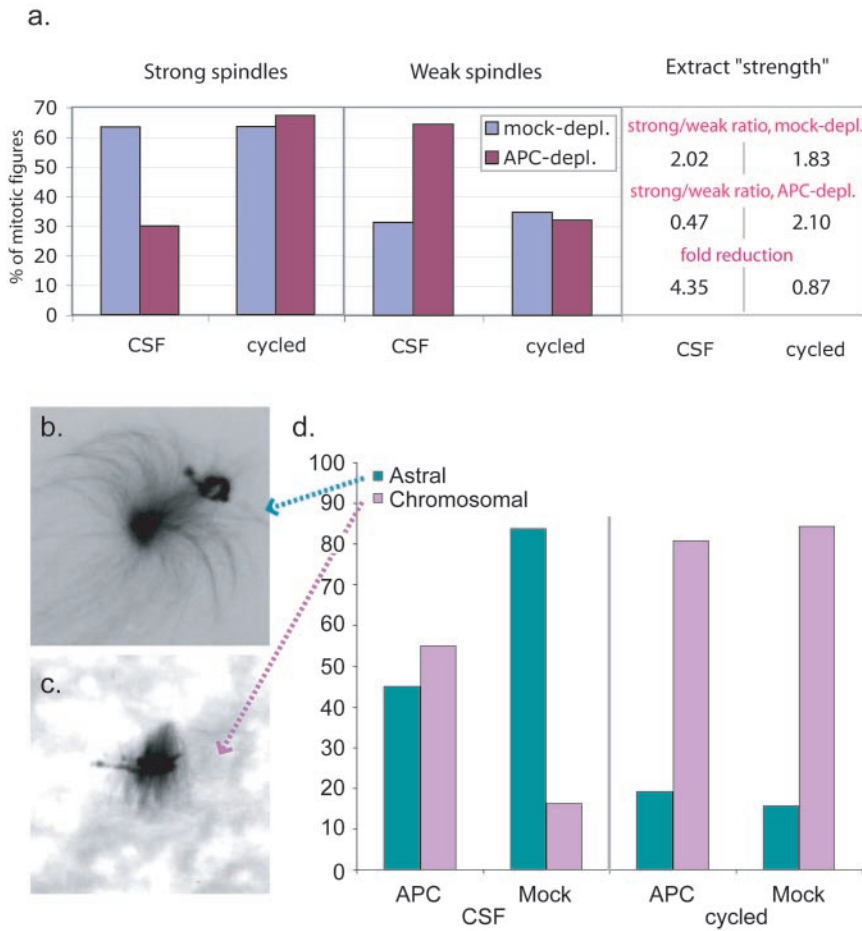


Figure 9. APC does not affect cycled spindle strength. (a) Spindles were formed in APC- and mock-depleted CSF or cycled extracts. The number of strong and weak spindles was counted as described for Figure 1. The histogram represents the % of strong and weak figures. Extract strength and fold reduction calculated as in Figure 1 are shown in the Table on the right. (b) Image of a typical “astral” and “chromosomal” (c) early mitotic figure. (d). The relative proportion of astral and chromosomal early mitotic figures are indicated for APC- and mock-depleted extracts before and after cycling. The y-axis represents the percent mitotic figures. In CSF extracts, astral figures predominated and APC depletion resulted in a reduction in their relative abundance. In cycled extracts, on the other hand, chromosomal asters were predominant, and APC depletion did not affect this distribution.

strong spindles before and after cycling through interphase and found that depleting APC did not compromise spindles formed in cycled extracts (Figure 9a).

In search for an explanation of these findings, we compared spindle intermediates formed in CSF and cycled extracts. Examination of microtubule structures at 10-min intervals during spindle assembly in CSF and cycled extracts revealed striking differences in the mode of spindle assembly (Figure 10). In CSF extracts, spindle assembly was commonly initiated from almost symmetrical asters in the vicinity of chromatin. At later times, asters had become polarized toward chromatin to form half spindles. A full spindle could then form by either joining of two such assemblies or by focusing the microtubules at the opposite side of chromatin. In contrast, the earliest structures observed during spindle assembly in cycled extracts were usually arrays of microtubules that emanated from well-condensed chromatin. At later time points, these microtubules became focused at their presumptive minus ends to form spindle poles and give rise to bipolar spindles. Only at late time points, when bipolar spindles had formed, aster-like structures could be observed near the poles of some of these spindles. These data confirmed previous studies describing two distinct pathways for spindle formation in CSF and cycled extracts (Sawin and Mitchison, 1991).

The most pronounced difference between these two types of extracts was the morphology of early mitotic figures: well-focused asters with microtubules polarized toward chromatin (“astral”) (Figures 9b and 10) or unfocused microtubule arrays concentrated around chromatin (“chromosomal”) (Figures 9c

and 10). These two types of early structures corresponded well to the two different mechanisms that have been described for nucleation of microtubules during spindle formation: radial microtubule nucleation at centrosomes or nucleation of a random microtubule array around chromatin (Hyman and Karsenti, 1998a; Scholey *et al.*, 2003). To quantitatively measure the relative contribution of these two mechanisms to spindle assembly in CSF and cycled extracts and also to determine whether APC selectively affected one of these mechanisms, we examined and classified early mitotic figures when approximately one-half of the assemblies had not yet formed bipolar spindles, in both APC-depleted and mock-depleted CSF and cycled extracts (Figure 9d). Due to the difference in the kinetics of spindle assembly in CSF and cycled extracts, this usually corresponded to 35 min in CSF extracts and 20 min in cycled extracts.

Counting the number of astral and chromosomal early mitotic figures confirmed that in mock-depleted CSF extracts, the majority of early assemblies were astral, indicating that in these extracts centrosome-directed spindle formation dominated. In contrast, in cycled extracts the chromosomal mitotic figures were most abundant. Consistent with the idea that the astral figures were specifically destabilized by APC depletion, the removal of APC shifted the proportion between astral and centrosomal microtubule structures toward chromosomally anchored figures (Figure 9d) in CSF extracts. Based on these findings, we suggest that APC specifically controls centrosome-directed spindle formation.

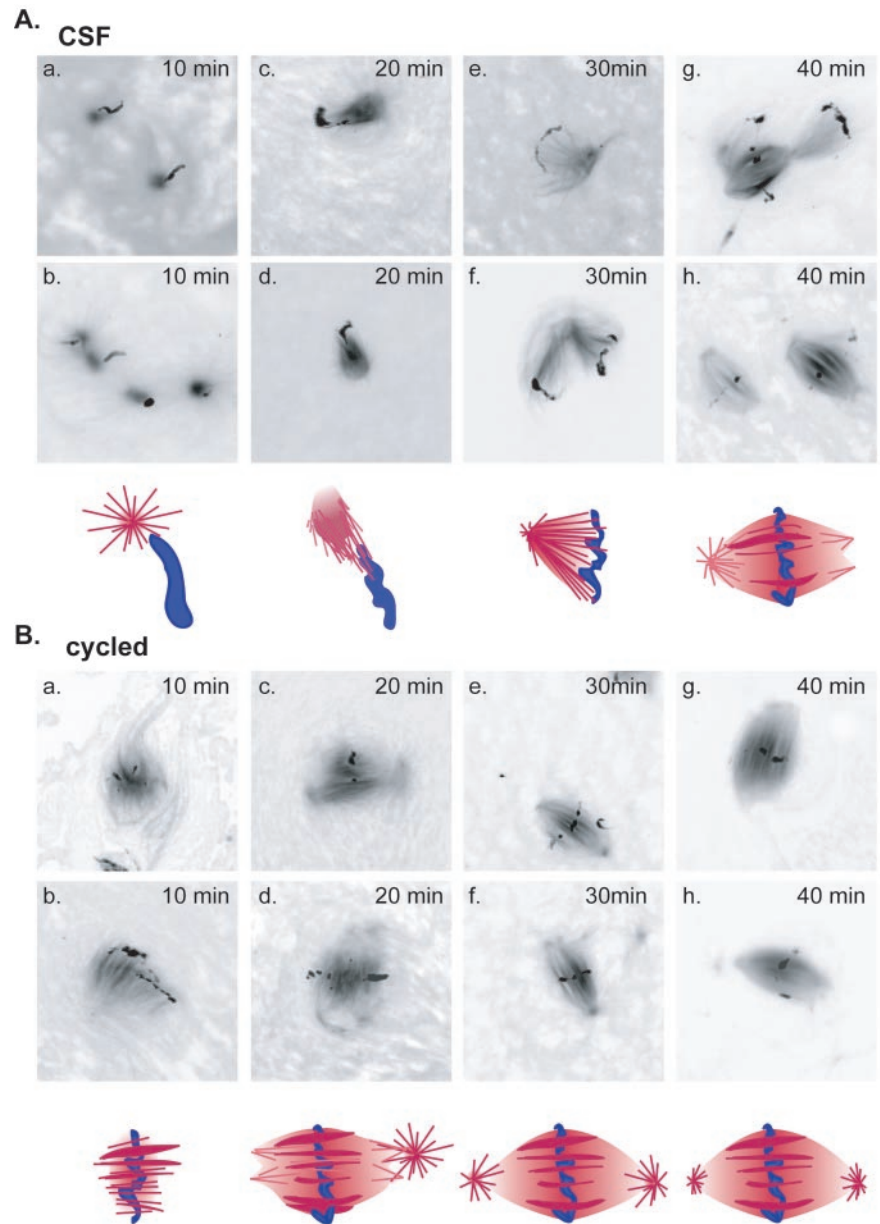


Figure 10. Formation of spindles in CSF and cycled extracts proceeds via different intermediates. Spindle formation was initiated in CSF (A) or cycled (B) extracts and microtubule structures examined every 10 min. Two examples of typical assemblies at each time point are displayed with a schematic representation of each of the intermediates shown below the corresponding images. In CSF extracts early intermediates were represented by asters that formed in the vicinity of chromatin and consisted of microtubules emanating from well focused points. By 20 min, these asters polarized toward the chromatin to form half spindles by 30 min. In cycled extracts, early intermediates were formed by chromatin from which microtubules emanated in parallel arrays. These arrays then reorganized to become more focused at their distal ends to form spindles.

DISCUSSION

Mutations in APC, a tumor suppressor protein with a well-established role in the regulation of β -catenin, are implicated in the development of chromosomal instability early in tumor formation (Shih *et al.*, 2001). We aimed to dissect the mechanism that allows APC to control chromosomal segregation. Specifically, we addressed whether loss of functional APC leads to spindle defects in mitosis. We took advantage of *Xenopus* egg extracts that are arrested in metaphase of meiosis II (CSF extracts) to monitor controlled spindle formation. We show that APC is required for the formation of robust spindles in such extracts, as APC removal reduced the microtubule content and altered the morphology of the microtubule network of spindles. This effect was rescued by addition of recombinant APC proteins, either full-length APC or a large, N-terminally truncated fragment. This rescue was dependent on the ability of APC to bind and stabilize microtubules. Our data support the direct involvement

of APC in spindle formation and implicate its interaction with microtubules in this function.

To interpret our data, the general mechanisms that govern spindle formation must be considered. There are two modes of spindle formation: chromosome directed and centrosome directed, and these modes are dependent on slightly different sets of components (Heald *et al.*, 1997; Hyman and Karsenti, 1998b). In accord with previous findings (Sawin and Mitchison, 1991), we established that cycled and noncycled (CSF) extracts differed in this respect. Monitoring the process of spindle formation in both extracts showed that in CSF extracts, centrosome-directed spindle formation dominated, whereas in cycled extracts spindles were assembled in a chromosome-directed manner (Figure 10). This was confirmed by determining the number of early spindle intermediates corresponding to each of these spindle formation modes. Furthermore, we observed that asters nucleated from exogenous centrosomes were formed less efficiently in cycled extracts than in CSF extracts (see Supplemental Figure 5), suggest-

ing that there is an intrinsic difference in the relative contribution and the kinetics of the two modes of spindle formation between these two types of extracts. This could produce a switch in the dominating mode of spindle assembly.

Remarkably, in cycled spindles, the weak spindle phenotype was not induced by APC depletion. Based on the difference found in the dominating mode of spindle formation between cycled and CSF extracts, we propose that APC is involved specifically in the regulation of centrosomally nucleated microtubules but may not be as important when microtubule nucleation is stimulated predominantly by chromosomes. In support of this idea, the relative contribution of centrosome- and chromosome-directed spindle formation in CSF extracts was shifted to the chromosome-directed spindle formation mode after removal of APC (Figure 9). The measurable contribution of chromosomally directed spindle formation in CSF extracts may account for the residual strong spindles in these extracts after APC depletion.

As suggested by Scholey *et al.* (2003) in centrosome-directed spindle formation, the main forces are generated by the interplay between dynamic microtubules that emanate from centrosomes and push spindle poles apart and counteracting forces provided by sliding microtubule motors that are localized to interpolar bundles. In this case, both of these forces determine spindle morphology and function. How do the pleiotropic effects we observed in APC-depleted spindles fit into this model? Our data led us to conclude that APC acts directly on microtubules to promote their outgrowth from centrosomes and stabilizes microtubule bundles. Stabilization of the microtubule lattice is important for a number of aspects of spindle structure and function and destabilization induced by APC depletion may explain the various effects we observed in APC-depleted spindles. In CSF extracts, the size of centrosome-nucleated asters and the length of assembled spindles were decreased in the absence of APC (Figures 2 and 8). The localization of APC to spindle poles further supports a role in establishing centrosomally anchored microtubule arrays.

Forces generated by interpolar microtubules may also be affected by APC depletion. The reduced amount of tubulin in the central spindle that is typical for APC-depleted spindles is consistent with the idea that there are fewer interpolar microtubule bundles in such spindles. The resulting decrease in the forces that hold such spindles together would make them more sensitive to external forces. Indeed, we found that APC-depleted spindles seemed to be more easily disrupted and often were pulled apart after centrifugation through a glycerol cushion. This observation also suggests that lack of APC may reduce microtubule cross-linking. The action of microtubule motors in the absence of efficient cross-linking could cause microtubule buckling, as predicted by Scholey *et al.* (2003). The wavy microtubules we commonly observed in APC-depleted spindles are consistent with this prediction (Figure 2).

In the context of centrosome-directed spindle formation, reduced microtubule length and rigidity induced by APC depletion could result in microtubules that are less efficient at reaching chromatin. This is supported by our observation that APC-depleted spindles have less tubulin in their midzone.

The localization of APC to kinetochores in cycled spindles (Figure 6) and in cells (Fodde *et al.*, 2001; Kaplan *et al.*, 2001) raises the possibility that APC also functions at kinetochores. Possible functions of APC at kinetochores include the participation in attachment of kinetochore fibers and/or stabilization of kinetochore fibers after attachment. In this case, removal of APC would result in the loss of microtubules from the kinetochore area, an idea that could provide

an alternative explanation for our observation that tubulin is redistributed toward spindle poles in APC-depleted spindles (Figure 3). However, general kinetochore structure seemed to be unaffected by the loss of APC, because the localization of the kinetochore proteins CenpE (Figure 6, e and f) and XKCM1 (our unpublished data) was not altered by removing APC. Defects in the dynamic attachment of microtubules to kinetochores normally results in misalignment of chromosomes (Wood *et al.*, 1997; Kline-Smith *et al.*, 2004). Chromosomes in APC-depleted spindles formed a metaphase plate; however, frequently a small portion of the DNA was found to extend beyond it (Supplemental Figure 6). As a consequence, we cannot exclude the possibility that APC has some function at kinetochores, but this function does not seem to be crucial for chromosome alignment in cycled extracts. More importantly, however, our data provide strong evidence for a kinetochore-independent function of APC in the formation of mitotic spindles that is related to its direct effect on microtubules themselves.

APC is a large protein with multiple binding partners (Dikovskaya *et al.*, 2001). It is conceivable that APC functions as a scaffold in the assembly of microtubule, centrosome, and/or kinetochore-associated proteins. A scaffolding role for APC is supported by the disruptive effect produced when a large C-terminal APC fragment is added in excess of endogenous APC (Figure 5). Excess full-length APC or an APC fragment may sequester essential proteins and disrupt protein complexes involved in spindle formation. Alternatively, the excessive growth of a subset of microtubules induced by an "overdose" of APC (Figure 8) could result in the destabilization of the spindle as a whole. These observations indicate that the effect of APC on spindles is normally controlled carefully. In this context, it is noteworthy that using known amounts of the purified APC4 fragment allowed us to estimate the concentration of endogenous APC protein in extracts. This yielded a concentration of approximately 10 nM, which is 10-fold lower than reported previously (Lee *et al.*, 2003).

Weakened spindles that result from loss of APC are more likely to lose their precious cargo because connections to chromatids might break during the segregation process. Thus, both the deterioration of microtubule attachment to kinetochores and the decrease in mechanical strength of the microtubule network upon loss of APC could result in aneuploidy. This is exactly what was found in cells carrying truncated APC and colorectal cancer cell lines stably transfected with truncated APC (Fodde *et al.*, 2001; Kaplan *et al.*, 2001; Green and Kaplan, 2003). Chromosomal missegregation in APC deficient cells suggests that these cells can successfully bypass the mitotic checkpoint that normally delays the separation of chromosomes until they are aligned correctly (Nigg, 2001). It is possible that in the weakened spindles induced by loss of APC, there is still sufficient tension and microtubule attachment at kinetochores to allow progression to anaphase without activating the checkpoint.

Even mild defects in chromosomal segregation, repeated each time a cell divides, will result in cumulative chromosomal instability, which in turn may accelerate the accumulation of tumorigenic mutations. Because gut epithelium is constantly being renewed, it relies heavily on mitotic fidelity. A role for APC in the formation of robust mitotic spindles may help to explain why mutations in APC accelerate tumor formation most prominently in this tissue.

ACKNOWLEDGMENTS

We thank all those who have contributed reagents as indicated in the manuscript. We are particularly grateful for help from Andreas Merdes (University of Edinburgh) with tubulin preparation. We thank all the members of the Näthke laboratory and Paul Clarke (University of Dundee) for helpful discussions and Jason R. Swedlow and members of his laboratory for help with extract preparation. D.D. is funded by a project grant from Cancer Research UK. I.S.N. is a Cancer Research UK Senior Research Fellow and a Burroughs Wellcome Career Development Awardee.

REFERENCES

- Bienz, M., and Clevers, H. (2000). Linking colorectal cancer to Wnt signaling. *Cell* 103, 311–320.
- Boland, C.R., and Kim, Y.S. (1993). Gastrointestinal polyposis syndromes. In: *Gastrointestinal Disease*, ed. M.H. Sleisinger and J.S. Fordtran, Philadelphia: WB Saunders, 1430–1436.
- Carazo-Salas, R.E., and Karsenti, E. (2003). Long-range communication between chromatin and microtubules in *Xenopus* egg extracts. *Curr. Biol.* 13, 1728–1733.
- Deka, J., Kuhlmann, J., and Muller, O. (1998). A domain within the tumor suppressor protein APC shows very similar biochemical properties as the microtubule-associated protein tau. *Eur. J. Biochem.* 253, 591–597.
- Desai, A., Murray, A.W., Mitchison, T.J., and Walczak, C.E. (1999). The use of *Xenopus* egg extracts to study mitotic spindle assembly and function in vitro. *Methods Cell Biol.* 61, 385–412.
- Dikovskaya, D., Zumburn, J., Penman, G.A., and Näthke, I.S. (2001). The Adenomatous Polyposis Coli protein: in the limelight out at the edge. *Trends Cell Biol.* 11, 378–384.
- Fearnhead, N.S., Britton, M.P., and Bodmer, W.F. (2001). The ABC of APC. *Hum. Mol. Genet.* 10, 721–733.
- Fodde, R., et al. (2001). Mutations in the APC tumour suppressor gene cause chromosomal instability. *Nat. Cell Biol.* 3, 433–438.
- Green, R.A., and Kaplan, K.B. (2003). Chromosome instability in colorectal tumor cells is associated with defects in microtubule plus-end attachments caused by a dominant mutation in APC. *J. Cell Biol.* 163, 949–961.
- Heald, R., Tournebise, R., Habermann, A., Karsenti, E., and Hyman, A. (1997). Spindle assembly in *Xenopus* egg extracts: Respective roles of centrosome and microtubule self-organisation. *J. Cell Biol.* 138, 615–628.
- Hyman, A., and Karsenti, E. (1998a). The role of nucleation in patterning microtubule networks. *J. Cell Sci.* 111, 2077–2083.
- Hyman, A.A., and Karsenti, E. (1998b). The role of nucleation in patterning microtubule networks. *J. Cell Sci.* 111, 2077–2083.
- Hyman, A.A., Drechsel, D., Kellogg, D., Salsler, S., Sawin, K., Pfeffen, P., Wordeman, L., and Mitchison, T.J. (1991). Preparations of modified tubulins. *Methods Enzymol.* 196, 478–485.
- Jimbo, T., Kawasaki, Y., Koyama, R., Sato, R., Takada, S., Haraguchi, K., and Akiyama, T. (2002). Identification of a link between the tumour suppressor APC and the kinesin superfamily. *Nat. Cell Biol.* 4, 323–327.
- Juwana, J.P., Henderikx, P., Mischo, A., Wadle, A., Fadle, N., Gerlach, K., Arends, J.W., Hoogenboom, H., Pfreundschuh, M., and Renner, C. (1999). EB/RP gene family encodes tubulin binding proteins. *Int. J. Cancer* 81, 275–284.
- Kaplan, K.B., Burds, A., Swedlow, J.R., Bekir, S.S., Sorger, P.K., and Näthke, I.S. (2001). A novel role for the APC tumour suppressor in chromosome segregation. *Nat. Cell Biol.* 3, 429–432.
- Kline-Smith, S.L., Khodjakov, A., Hergert, P., and Walczak, C.E. (2004). Depletion of centromeric MCAK leads to chromosome congression and segregation defects due to improper kinetochore attachments. *Mol. Biol. Cell* 15, 1146–1159.
- Lee, E., Salic, A., Kruger, R., Heinrich, R., and Kirschner, M.W. (2003). The roles of APC and axin derived from experimental and theoretical analysis of the Wnt pathway. *PLoS Biol.* 1, E10.
- Louie, R.K., Bahmanyar, S., Siemers, K.A., Votin, V., Chang, P., Stearns, T., Nelson, W.J., Barth, A.I. (2004). Adenomatous polyposis coli and EB1 localize in close proximity of the mother centriole and EB1 is a functional component of centrosomes. *J. Cell Sci.* 117, 1117–1128.
- Murray, A.W. (1991). Cell cycle extracts. *Methods Cell Biol.* 36, 581–605.
- Näthke, I.S., Adams, C.L., Polakis, P., Sellin, J.H., and Nelson, W.J. (1996). The adenomatous polyposis coli tumor suppressor protein localizes to plasma membrane sites involved in active cell migration. *J. Cell Biol.* 134, 165–179.
- Nigg, E.A. (2001). Mitotic kinases as regulators of cell division and its checkpoints. *Nat. Rev. Mol. Cell Biol.* 2, 21–32.
- Polakis, P. (1997). The adenomatous polyposis coli (APC) tumor suppressor. *Biochim. Biophys. Acta* 1332, F127–F147.
- Polakis, P. (2001). More than one way to skin a catenin. *Cell* 105, 563–566.
- Sawin, K.E., and Mitchison, T.J. (1991). Mitotic spindle assembly by two different pathways in vitro. *J. Cell Biol.* 112, 925–940.
- Scholey, J.M., Brust-Mascher, I., and Mogilner, A. (2003). Cell division. *Nature* 422, 746–752.
- Shih, I.M., Zhou, W., Goodman, S.N., Lengauer, C., Kinzler, K.W., and Vogelstein, B. (2001). Evidence that genetic instability occurs at an early stage of colorectal tumorigenesis. *Cancer Res.* 61, 818–822.
- Su, L.-K., Burrell, M., Hill, D.E., Gyuris, J., Brent, R., Wiltshire, R., Trent, J., Vogelstein, B., and Kinzler, K.W. (1995). APC binds to the novel protein EB1. *Cancer Res.* 55, 2972–2977.
- Swedlow, J.R. (1999). Chromosome assembly in vitro using *Xenopus* egg extracts. In: *Chromosome Analysis*, ed. W. Bickmore, Oxford: Oxford University Press, 165–182.
- Tighe, A., Johnson, V.L., Albertella, M., and Taylor, S.S. (2001). Aneuploid colon cancer cells have a robust spindle checkpoint. *EMBO Rep.* 2, 609–614.
- Tirnauer, J.S., Grego, S., Salmon, E.D., and Mitchison, T.J. (2002). EB1-microtubule interactions in *Xenopus* egg extracts: role of EB1 in microtubule stabilization and mechanisms of targeting to microtubules. *Mol. Biol. Cell* 13, 3614–3626.
- Wood, K.W., Sakowicz, R., Goldstein, L.S., and Cleveland, D.W. (1997). CENP-E is a plus end-directed kinetochore motor required for metaphase chromosome alignment. *Cell* 91, 357–366.
- Zumburn, J., Inoshita, K., Hyman, A.A., and Näthke, I.S. (2001). Binding of the Adenomatous Polyposis Coli protein to microtubules increases microtubule stability and is regulated by GSK3b phosphorylation. *Curr. Biol.* 11, 44–49.